Serological Assays Estimate Highly Variable SARS-CoV-2 Neutralizing Antibody Activity in Recovered COVID19 Patients

Larry L. Luchsinger,[a,#] Brett Ransegnola,[a] Daniel Jin,[a] Frauke Muecksch,[b] Yiska Weisblum,[b] Weili Bao,[d] Parakkal Jovvian George,[e] Marilis Rodriguez,[f] Nancy Tricoche,[e] Fabian Schmidt,[b] Chengjie Gao,[g] Shabnam Jawahar,[e] Mouli Pal,[d] Emily Schnall,[e] Huan Zhang,[g] Donna Strauss,[h] Karina Yazdanbakhsh,[d] Christopher D. Hillyer,[a,h] Paul D. Bieniasz,[b,c,#] Theodora Hatziioannou,[b,#]

[a.] Laboratory of Stem Cell Regenerative Research, Lindsley F. Kimball Research Institute, New York Blood Center, New York, NY 10065, USA.
[b.] Laboratory of Retrovirology, The Rockefeller University, New York, NY 10065, USA
[c.] Howard Hughes Medical Institute, New York, NY 10016, USA.
[d.] Laboratory of Complement Biology, Lindsley F. Kimball Research Institute, New York Blood Center, New York, NY 10065, USA.
[e.] Laboratory of Molecular Parasitology Lindsley F. Kimball Research Institute, New York Blood Center, New York, NY 10065, USA.
[f.] Laboratory of Blood-Borne Parasites, Lindsley F. Kimball Research Institute, New York Blood Center, New York, NY 10065, USA.
[g.] Laboratory of Membrane Biology, Lindsley F. Kimball Research Institute, New York Blood Center, New York, NY 10065, USA.
[h.] New York Blood Center Enterprises, New York, NY 10065, USA.
[i.] Equal authorship
\# Co-corresponding authors

Running Head: Covid19 Serology Result Predict Neutralizing Activity

Address correspondence to Larry Luchsinger (Lead): lluchsinger@nybc.org

Abstract

The development of neutralizing antibodies (nAb) against SARS-CoV-2, following infection or vaccination, is likely to be critical for the development of sufficient population immunity to drive cessation of the COVID19 pandemic. A large number of serologic tests, platforms and methodologies are being employed to determine seroprevalence in populations to select convalescent plasmas for therapeutic trials, and to guide policies about reopening. However, tests have substantial variability in sensitivity and specificity, and their ability to quantitatively predict levels of nAb is unknown. We collected 370 unique donors enrolled in the New York Blood Center Convalescent Plasma Program between April and May of 2020. We measured levels of antibodies in convalescent plasma using commercially available SARS-CoV-2 detection tests and in-house ELISA assays and correlated serological measurements with nAb activity measured using pseudotyped virus particles, which offer the most informative assessment of antiviral activity of patient sera against viral infection. Our data show that a large proportion of convalescent plasma samples have modest antibody levels and that commercially available tests have varying degrees of accuracy in predicting nAb activity. We found the Ortho Anti-SARS-CoV-2 Total Ig and IgG high throughput serological assays (HTSAs), as well as the Abbott SARS-CoV-2 IgG assay, quantify levels of antibodies that strongly correlate with nAb assays and are consistent with gold-standard ELISA assay results. These findings provide immediate clinical relevance to serology results that can be equated to nAb activity and could serve as a valuable 'roadmap' to guide the choice and interpretation of serological tests for SARS-CoV-2.

48 **Introduction**

49 In late 2019, a cluster of patients in Wuhan, the capital city of China's Hubei providence, were
50 reported to be afflicted with a severe respiratory illness of unknown origin.(1, 2) Patients presented with
51 symptoms that included high fever, pneumonia, dyspnea, and respiratory failure. The causative agent was
52 identified to be severe acute respiratory syndrome coronavirus variant 2 (SARS-CoV-2), the 7th coronavirus
53 strain to infect humans to date,(3) and the clinical syndrome was designated coronavirus disease of 2019
54 (COVID19). The pathogenesis of COVID19 is similar to previously documented respiratory distress
55 syndromes caused by related coronaviruses, including the 2005 SARS coronavirus (SARS-CoV) and the
56 middle east respiratory syndrome coronavirus (MERS).(4) However, the greater transmissibility of SARS-
57 CoV-2 has enabled a swift global spread that has resulted in substantial mortality. Detection and tracking
58 SARS-CoV-2 spread has been difficult. Moreover, the spectrum of symptomatology observed in SARS-
59 CoV-2 infection is wide, ranging from asymptomatic and mild, reminiscent of numerous seasonal
60 infections, including influenza and common cold viruses, all the way to life-threatening respiratory failure
61 that requires intensive care and invasive ventilation. Currently, increased age and comorbidities are the
62 factors most highly predictive of severe of COVID19 disease.(5)

63 The utility of serological tests to identify individuals who have acquired antibodies against SARS-
64 CoV-2 is thus recognized as both an indication of the seroprevalence of SARS-CoV-2 infection and,
65 potentially, of immunity afforded to the seropositive individual.(3, 6-8) Seroconversion is determined by
66 detection of antibodies that recognize SARS-CoV-2 antigens. Coronaviruses have 4 major structural
67 proteins: spike (S) protein (including the S1 protein and receptor binding domain (RBD)), nucleocapsid (N)
68 protein, membrane (M) protein and envelope (E) protein.(9) Previous studies of SARS-CoV and MERS
69 found the most immunogenic antigens are the S- and N-proteins,(10) and development of serological tests
70 for SARS-CoV-2 antibodies has focused heavily on these viral proteins.

71 Three major platforms of serological testing have been adopted; 1) enzyme linked immunosorbent
72 assays (ELISA), 2) high-throughput serological assays (HTSA), and 3) lateral flow assays (LFA). ELISAs
73 offer wide flexibility for research laboratories to select virtually any antigen of interest and provide highly

74 sensitive, quantitative results. HTSAs are more suitable for clinical laboratories and offer limited antigen
75 diversity but allow high-throughput and sensitive, semi-quantitative results. LFAs also offer limited
76 antigen diversity, but function with small volumes (~20μL) of whole blood, plasma or sera and allow rapid
77 (≤15 minutes) results at the point of care. The clinical community will undoubtedly employ multiple
78 SARS-CoV-2 serology platforms but a comparative analysis across platforms has not been undertaken.
79 Further, it is currently unknown whether the detection of antibodies that bind these proteins predicts
80 neutralizing activity or protection against infection.(11)

81 Convalescent plasma (CP) transfusion has been recognized as a potential treatment for critically ill
82 COVID19 patients and the New York Blood Center (NYBC) has led the first COVID19 CP donation
83 program in the United States. Using 370 unique CP donor samples deposited in our COVID19 Research
84 Repository (https://nybc.org/covid19repository), we conducted ELISA, HSTA and LFA assays as well as
85 SARS-CoV-2 pseudovirus neutralization assays. We find that CP donors have a wide range of antibody
86 titers measured across multiple COVID19 serological and neutralization assays. Notably, we show that
87 some HTSA and ELISA assays predict neutralizing activity *in vitro* and may thus serve to predict antiviral
88 activity against SARS-CoV-2 *in vivo*.

89 **Results**

90 **Characteristics of the NYC CP Donor Population**

91 Serological analysis of the CP donors was performed using 370 unique samples collected between
92 April and May of 2020 from the NYC area. CP donors enrolled in the program were required to have tested
93 positive for SARS-CoV-2 by PCR diagnostic tests and be symptom free for at least 2 weeks. To profile CP
94 donors, we cross-referenced donor demographic data to the 2010 U.S. Census database.(12) CP donors had
95 a median age of 41 years (95% CI: 39-44, range 17-75 years,) and showed a gaussian distribution (n=183,
96 r^2=0.89) compared to the national median age of 38.2 years in 2018 (**Figure 1A**). The frequency of male
97 and female CP donors was 45.2% and 54.8%, respectively, and was not statistically different from the
98 national average of 49.2% and 50.8% (**Figure 1B**). The frequency of ABORh blood group antigens was
99 also largely consistent with the national frequency, with a slightly higher number of A^- and O^- donors and

100 slightly lower number of AB^+ and B^+ donors than expected (**Figure 1C**). Finally, CP donor ethnicity was
101 largely consistent with the national ethnic composition, with a slightly higher number of multiracial/other
102 donors and lower number of Black/African American donors than expected (**Figure 1D**). Overall, the
103 composition of NYC CP donors analyzed was reflective of the United States population demographic.

104 **Neutralizing Activity of the CP Donor Population**

105 Neutralization assays measure how effectively donor plasma or serum can inhibit virus infection of
106 target cells and are the gold standard for measuring the antiviral activity of antibodies. In the case of SARS-
107 CoV-2, such assays require in biosafety level 3 (BSL-3) facilities and highly trained personnel. To
108 overcome this limitation and expedite testing, we employed pseudotyped virus assays based on either HIV-
109 1 (human immunodeficiency virus type 1) or VSV (vesicular stomatitis virus). Both viruses were
110 engineered to lack their own envelope glycoproteins and to express a luciferase reporter gene.
111 Complementation *in trans* with the SARS-CoV-2 Spike (S) protein results in the generation of pseudotyped
112 virus particles that are dependent on the interaction between the S protein and its receptor ACE2
113 (angiotensin-converting enzyme 2) for entry into cells.(13) These reporter viruses were used to measure
114 infection of human cells engineered to express ACE2 (HIV-S assay) or expressed endogenous ACE2
115 (VSV-S assay) and to determine the ability of plasma dilutions to inhibit S-dependent virus entry. The NT_{50}
116 values, reflecting the plasma dilution at which virus infection is reduced by 50%, were calculated for each
117 sample (**Supplementary Figure 1A**).

118 The neutralizing activity of CP donor samples was extremely variable and NT_{50} values obtained
119 ranged from <50 to over 20,000. The median NT_{50} values were 390.1 (95% CI: 278.3-499.7) and 450.6
120 (95% CI: 367.7-538.4) for the HIV-S or VSV-S assays, respectively (**Figure 2A**) and the two assays
121 showed a high degree of correlation (**Supplementary Figure 1B-C**). Fresh frozen plasma (FFP) samples
122 donated in 2019, before the SARS-CoV-2 outbreak, were used as negative controls (n=10). Importantly, the
123 NT_{50} values of all FFP samples were ≤50, which is the highest concentration of plasma used in the
124 neutralization assays and is hence designated as the signal cutoff (S/co) value. Overall, 83.1% and 92.7% of
125 the CP donor samples had detectable neutralization activity using HIV-S and VSV-S assays, respectively

126 (**Figure 2B**). Notably, 11.2% and 8.7% of CP donors had NT_{50} values at or greater than 2000 (40-fold over
127 S/co) using HIV-S and VSV-S, assays respectively while 55.8% and 52% of CP donors had NT_{50} values at
128 or less than 500 (10-fold over S/co) (**Figure 2B**). Thus, the majority of CP donors may have relatively
129 modest neutralizing activity and a small proportion of donors have high neutralization activity.

130 NT_{50} values were not statistically different between blood groups (**Figure 2E, Supplementary**
131 **Figure 1G**) or age groups (**Figure 2C, Supplementary Figure 1E**) and there was no linear correlation of
132 NT_{50} values with age (**Supplementary Figure 1D**) in contrast to previous reports.(14) However, in
133 agreement with recent studies,(15) NT_{50} values of male CP donor samples were ~1.7-fold higher than those
134 from female CP donors using HIV-S and VSV-S assays (**Figure 2D and Supplementary Figure 1F,** n =
135 195, p = 0.009 and <0.001, median difference 217 and 197, respectively). For CP donors where symptom
136 dates were reported, the time between last symptom and the date of donation was calculated. Interestingly,
137 CP donors 2-3 weeks post symptoms had a statistically significant increase in NT_{50} values compared to CP
138 donors >3 weeks post-symptom (**Figure 2F and Supplementary Figure 1H,** n=52, p = 0.03 and 0.04,
139 median difference 426 and 226, respectively). Overall, these data suggest CP donors possess a wide range
140 of neutralizing antibody levels that are proportionately distributed across demographic categories with the
141 exception of a small sex-dependent effect.

142 **Serological Test Results of the CP Donor Population**

143 Multiple platforms have been deployed to detect seroconversion against SARS-CoV-2. The
144 simplest tests are LFAs, which solubilize antibodies from whole blood, plasma or sera in an aqueous
145 mobile phase which moves across a nitrocellulose membrane coated with anti-human IgG and/or IgM to
146 distinguish between specific classes of immunoglobins while a control band ensures test function. Binding
147 of antibodies to antigen-conjugated enzyme, such as horseradish peroxidase, generates a colored band at
148 the test lines. Analysis of 144 CP donor samples showed that only 79.4% of CP donors tested positive for
149 SARS-CoV-2-specfic IgG antibodies and 24.8% for IgM antibodies (**Figure 3A, top**). While LFAs are not
150 designed to perform quantitatively, large discrepancies in band intensity between donors (**Supplementary**
151 **Figure 2A**) is often presumed to indicate semi-quantitative results. We performed densitometric analysis of

152 the test bands from LFA cassettes (**Supplementary Figure 2B, 2C**) and normalized each test to control
153 band intensity. LFAs showed an intensity range of 0% - 99.2% for IgG bands and 0% - 18.5% for IgM
154 bands, with a median intensity of 20% for IgG and <1% for IgM (**Figure 3A, bottom**). Thus, LFAs have a
155 high degree of variation in band intensity within the CP donor population.

156 HTSA systems offer the advantage of performing semi-quantitative seroconversion assays using
157 clinical laboratory testing infrastructure at large scale. We performed the Ortho-Clinical Diagnostics
158 VITROS SARS-CoV-2 total Ig assay, the VITROS SARS-CoV-2 IgG assay and the Abbott Labs Architect
159 SARS-CoV-2 IgG assay using between 100 and 330 CP donor plasma samples. We found 96.4% and
160 91.0% of CP donor samples were positive using the Ortho total Ig and IgG assays, respectively, and 91.4%
161 were positive using the Abbott IgG assay (**Figure 3B**). The median value of CP samples using the Ortho
162 total Ig assay was 101 arbitrary units (AU) (n=333, 95% CI: 78.5 – 123, S/co = 1, range 0 to 1000 AU)
163 while that of FFP healthy controls was 0.01 AU (n=8, 95% CI: 0.01 – 0.02). Similarly, the median value of
164 CP samples using the Ortho IgG assay was 11.7 AU (n=100, 95% CI: 8.3 – 16.07, S/co = 1, range 0 to ~30
165 AU). For the Abbott assay, the median value of CP samples was 6.04 AU (n=315, 95% CI: 5.48 – 6.44,
166 S/co = 1.4, range 0 to ~10 AU) while that of FFP healthy controls was 0.02 AU (95% CI: 0.01 – 0.15).
167 These results clearly show HTSA platforms detect a wide variation in antibody levels in the CP donor
168 population and offer greater dynamic range than LFA assays.

169 The gold standard for quantification of antigen-specific antibodies is ELISA assays. Studies of
170 antibody responses during SARS-CoV and MERS outbreaks identified the S- and N-proteins as the
171 dominant antigens. Therefore, we designed three indirect ELISA assays using SARS-CoV-2 recombinant,
172 His-tagged, spike protein S1 domain (S1), spike protein RBD domain (RBD) and nucleocapsid protein (N).
173 We utilized monoclonal antibodies demonstrated to bind antigen in a dose-dependent manner to generate
174 standard curves from which antibody concentrations were calculated and FFP from healthy controls to
175 determine signal cutoffs. Thus, we report our ELISA results as monoclonal antibody (mAb) titers. These
176 ELISA assays showed that 85.2%, 89.1%, and 96.3% of CP donor samples were positive for antibodies
177 against S1, RBD and N antigens, respectively (**Figure 3C**). Using the S1 ELISA, the median value for CP

178 donor samples was 445μg/mL (n=285, 95% CI: 342 – 536μg/mL, S/co = 120μg/mL) and for FFP controls
179 100.9μg/mL (n=10, 95% CI: 78 – 120μg/mL). In the NP ELISA the median value for CP donor samples
180 was 6432μg/mL (n=271, 95% CI: 2811 – 13792μg/mL, S/co = 700μg/mL) while in the RBD ELISA the
181 median value of CP donor samples was 15.6μg/mL (n=43, 95% CI: 12.55 – 25.6μg/mL, S/co = 4μg/mL).
182 Notably, the range of S1 and NP-binding antibody concentrations observed in the ELISAs was extreme,
183 constituting a 1,000-fold difference in titers within the CP donor population. Taken together, these data
184 demonstrate that CP donors have a wide range of concentrations of antibodies specific to immunogenic
185 SARS-CoV-2 antigens, as measured across multiple serological platforms.

186 **Correlation of Serology Tests with Neutralizing Activity**

187 It is not logistically feasible to implement neutralization assays as a measurement of antiviral
188 antibodies at a scale of the general population. While quantification of seroconversion is practiced,
189 controlled studies that determine the relationship between quantitative SARS-CoV-2 serology test results
190 and neutralizing activity is sparse. We examined the correlation between serology and neutralization assays
191 in the CP donor samples (**Figure 4A, Supplementary Figure 3A, Supplementary Figure 4C**). As
192 expected, S1 ELISA titers showed a positive linear regression with NT_{50} values ($r^2 = 0.35$) while the RBD
193 ELISA titers showed slightly higher linearity ($r^2 = 0.38$), commensurate with the fact that the RBD is a key
194 target for neutralizing antibodies. Conversely, NP ELISA titers showed a comparatively lower degree of
195 linear regression with neutralization activity ($r^2 = 0.09$). By comparison, both the Ortho HTSA total Ig
196 assay and the IgG assay showed higher ($r^2 = 0.45$ for both) while the Abbott HTSA IgG assay showed
197 lower linear regression with neutralization activity ($r^2 = 0.24$). Although Ortho HTSAs and the Abbott
198 HTSA IgG platforms quantify antibodies against S1 and NP antigens, respectively, a linear regression of
199 r^2=0.33 was calculated between these two HTSAs (**Supplementary Figure 3B**). As expected, linear
200 regression between the Ortho total Ig and IgG assay was strong ($r^2 = 0.72$) since the two assays measure the
201 same epitope. LFA IgG densitometry measurements showed the poorest correlation with neutralization
202 activity ($r^2 = 0.22$).

203 Correlation between serological results and neutralization activity was also examined using the non-
204 parametric Spearman test that does not assume linear dependence (**Figure 4B**). As expected, a high
205 correlation between the HIV-S and VSV-S neutralization assays was obtained (r=0.89). The Ortho and
206 Abbott HTSA platforms exhibited the highest degree of correlation with neutralization among the serology
207 assays tested (r = 0.75 and 0.72, respectively for the HIV-S assay; 0.70 and 0.69 for the VSV-S assay). The
208 S1, RBD, and NP ELISAs also showed a high degree of correlation, particularly with the HIV-S
209 neutralization assay (r = 0.69, 0.65, and 0.65) while the LFA IgG and IgM assay showed the poorest
210 correlation (r = 0.56, 0.41). Taken together, the data demonstrate that all quantitative serological assays
211 correlate to some degree with neutralization activity. However, HTSA and S1 ELISA assays that measure
212 anti-spike protein antigens have the highest predictive value as a surrogate for pseudovirus neutralization
213 assays. Importantly, correlation between HTSA scores and NT_{50} values suggest presumptive ranges of
214 neutralizing activity based on ranges of HTSA values (**Figure 4C, Supplementary Figure 4A**).
215 While ELISA assays revealed S1 and N antibody titers correlated with each other, these titers were
216 not always proportional among CP donor samples. To examine the coincidence of S1 and NP antibody
217 titers and using FFP plasma samples as negative controls, we categorized S1 and N antibody titers that fell
218 below S/co values as 'negative' and titers greater 10-fold over S/co as 'high' (**Supplementary Figure 4B**).
219 Using 241 CP donor samples that were assayed with both the S1 and N ELISA assays, we found that 81%
220 of donors were double positive (DP), while 16% of samples were single positive (14% N and 2% S1,
221 respectively) (**Figure 4D**). Only 2.5% of CP donors were double negative for S1 and NP antibodies. Within
222 the double positive population, we found that 23% of samples were DP^{high} while 5% and 30% of samples
223 were only $S1^{high}$ or N^{high} and the remaining 42% were DP^{low}. We then examined the distribution of NT_{50}
224 values from the HIV-S neutralization assay within these populations (**Figure 4E**). Notably, DN samples
225 showed NT_{50} values at the S/co observed for FFP healthy control samples while DP^{low} samples had
226 relatively low NT_{50} values (median value 327, 95% CI: 186 – 444). Importantly, the DP^{high} donors had
227 NT_{50} values that were 7-fold higher than DP^{low} donors (median value 2130). Additionally, NT_{50} values in
228 the N^{high} and $S1^{high}$ groups were 2.5- and 4-fold higher than those of the DP^{low} group.

229 Finally, we sought to determine if the frequency of peripheral blood immune cells varied as a
230 function of antibody titer. We stained peripheral blood mononuclear cells (PBMCs) isolated from CP donor
231 buffy coats for classical surface markers associated with B-cell or T-cell populations (**Supplementary**
232 **Figure 5A, 5B**). We examined T cell subsets including T central memory (CD45RO+CD62L+) and T
233 effector memory (TEM; $CD45RO^{+}CD62L^{neg}$) while B cell ($CD20^{+}$) subsets analyzed included memory B
234 cells ($CD27^{+}CD24^{+}$), plasmablasts ($CD24^{neg}CD38^{hi}CD138^{neg}$) and the more mature plasma cells
235 ($CD24^{neg}CD38^{hi}CD138^{+}$) (**Supplementary Figure 5C**). We found statistically significant differences in
236 naïve CD4 and CD8 T-cell populations in donors with high S1 ELISA titers compared to those with low
237 titer. Decrease in $CD24^{+}CD27^{+}$ memory B cells was detected in individuals with higher anti-S titers.
238 Although the cause of this lower frequency is not known, it could raise the possibility that individuals with
239 reduced memory B cells may develop a less robust antibody response with future infections. Although our
240 phenotypic analysis of B and T cell compartments was limited, these data suggest phenotypic differences in
241 canonical B and T cell populations are insufficient to explain the large differences in antibody titers or
242 neutralization activity observed in CP donors and warrants future studies designed to study B and T cell
243 function from individual donors.

244 **Discussion**

245 **Demographic limitations of the CP donor population**

246 Recent studies have noted a disproportion in COVID19 morbidity and mortality among minority
247 communities.(16) In this study, of the 370 CP samples analyzed, only 204 donors (55%) elected to identify
248 ethnicity, representing the least reported demographic category we collected. Nevertheless, we did not
249 observe a significant difference in nAb or serology results as a function of any demographic metric,
250 including ethnicity. Although we showed that the CP donor samples analyzed in this study comprised a
251 relatively normal distribution of demographic indicators, based on the U.S. census data, we acknowledge
252 that some factors, including ethnicity, are underrepresented in this cohort and limit the interpretation of the
253 study beyond the population aggregate. The potential explanations of this phenomenon are complex and
254 extend beyond the scope of this study.(17) The blood banking community is continuously working to

255 recruit minority donors, who are consistently underrepresented amongst regular blood donors.(18) Efforts
256 to increase public participation in local blood and CP donor programs would both improve blood product
257 diversity of transfusion products and strengthen the rigor of epidemiological disease. Thus, studies
258 designed to characterize serological responses to COVID19 specifically in minority groups are warranted
259 and necessary to augment our current understanding of the pandemic.

260 **Seroconversion assays of the population**

261 Quantification of antiviral antibodies in recovered individuals is an important metric for
262 determining population immunity conferred by exposure to SARS-CoV-2. Our study suggests that most
263 New York City convalescent plasma donors have antibodies against SARS-CoV-2. Indeed, our data
264 demonstrate that the HTSA, including Ortho and Abbot assays, which have received EUA from the FDA,
265 are well suited to quantify a wide range of antibody titers and reported that 91 – 96.4% of the CP
266 population possesses detectable SARS-CoV-2 antibodies. LFAs performed less well, and individuals with
267 low antibody titers scored weakly positive or negative in LFAs. Such outcomes could be interpreted
268 incorrectly, thus increasing the rate of false negative results. Ultimately, studies that accurately document
269 SARS-CoV-2 seroprevalence in diverse populations will require highly sensitive, high quality assays such
270 as HSTA or ELISA to be reliable.

271 **Correlation between serological assay measurements and neutralizing activity**

272 Since patient recovery often precedes the development of efficacious and safe therapeutics, a
273 longstanding treatment strategy for infectious diseases is passive antibody transfer. Therefore, refining
274 strategies to improve CP infusion efficacy benefits both the current treatment options of COVID-19 and
275 will inform the medical community for future pandemics. Our serological analyses are consistent with
276 previous publications that show a considerable range in antibody titers in recovered COVID19 patients.(19)
277 However, this study provides a comprehensive analysis of the correlation of quantitative serological test
278 values with neutralization activity. Importantly, high dynamic range serological assays, such as the HTSA
279 and S1 ELISA, had a significant linear correlation with neutralization activity. We show, for the first time,
280 the extent to which three widely available SARS-CoV-2 HTSAs correlated to nAb activity as well as to

281 each other, providing the clinical and scientific community with a comprehensive overview of clinical
282 serology test performance. To this end, investigators from the Mayo Clinic's COVID-19 Expanded Access
283 Program (EAP) performed an exploratory analysis on the efficacy of CP as a therapeutic agent using data
284 from over 35,000 transfusions.(20) Although the study showed uncertainty as to the statistical significance
285 of effect, the authors noted that patients transfused with high antibody titer CP units, quantified by the
286 Ortho IgG assay, showed a notable reduction in the odds ratio of mortality at both 7 and 30 days after
287 transfusion. These data support the assertion that antibody quantification of CP units using high dynamic
288 range HSTA assays may further improve therapeutic options for COVID-19 and, perhaps, future pandemic
289 responses. This knowledge will also be necessary for deriving potential serologic correlates of
290 protection,(21) and may aid in predicting immunity at the individual and population levels.(15)
291 Yet, the levels of plasma neutralizing activity required to prevent SARS-CoV-2 re-infection are
292 currently unknown. Anecdotal results have been reported for seasonal coronavirus experimental infection
293 studies. For example, one study of 229E HCoV found a positive correlation between pre-infection antibody
294 titer and neutralization activity with symptom clinical severity.(22) In another study, 7 of 8 individuals with
295 low neutralizing titers excreted virus upon re-exposure, compared to only 1 of 4 subjects with higher
296 titers.(23) However, the conclusions of these studies are not directly comparable to the current SARS-CoV-
297 2 pandemic. As such, the necessity of human epidemiological or vaccination studies are necessary to
298 determine the minimum threshold of neutralizing activity necessary to prevent SARS-CoV-2 re-infection.
299 Conversely, sub-neutralizing antibody levels have been reported to facilitate, rather than inhibit, viral entry
300 of the some coronaviruses *in vitro*, through antibody dependent enhancement (ADE).(24-26) While ADE
301 dependent replication has not been demonstrated to occur in SARS-CoV, viral uptake into macrophages via
302 antibody association with Fc receptors does induce IL-6 and TNFα cytokines which may promote
303 inflammation and tissue damage.(27) Insights gained from an accurate analysis of antibody levels and
304 neutralization activity in SARS-CoV-2-infected individuals will help address these important questions and
305 the corresponding health consequences.

306 A key biological question is: what underlies the large variation in antibody titers (neutralizing or
307 otherwise) observed in CP donors? Numerous variables, including the effectiveness of innate immune
308 responses, SARS-CoV-2 exposure dose, anatomical site of initial infection, and partial cross-reactive
309 immunity conferred by prior seasonal coronavirus infection, could all impart variation on the amount and
310 dissemination of SARS-CoV-2 antigen. Variation in the exposure of the adaptive immune system to SARS-
311 CoV-2 antigen would, in turn, likely impact the magnitude of immune responses. Our observation that the
312 levels of antibody to N, as well as S, correlates with S-specific neutralizing titer suggests that quantitative
313 differences in the overall adaptive immune response to SARS-CoV-2, rather than intrinsic differences in
314 the ability of individuals to mount neutralizing responses, at least partly explains the large variation in
315 neutralizing capacity of CP. This notion is consistent with recent findings that all individuals examined,
316 generated very similar, potent monoclonal SARS-CoV-2 neutralizing antibodies, but at very different
317 levels.(15)

318 **Future utility for vaccine and CP donor strategies**

319 The development of efficacious vaccines against SARS-CoV-2 may be necessary for ending the
320 COVID19 pandemic. Clinical trials will undoubtedly include a battery of serological and neutralization
321 assays in test subjects to assess candidate vaccine efficacy. Surrogate serology tests to neutralizing activity
322 could help to rapidly inform as to the likely effectiveness, as well as immunogenicity, of vaccines against
323 SARS-CoV-2. To this end, real-time analyses using scalable HTSA testing platforms is effectuate while
324 future studies are conducted to more precisely measure *in vivo* neutralization activity.

325 Finally, the utility of convalescent plasma in the treatment of infection has been recognized since
326 the turn of the 20th century.(28) CP transfusion is thought to be effective through passive immunization,
327 specifically the transfer of neutralizing antibodies from a recovered individual to another individual
328 manifesting life-threatening symptoms.(29, 30) Previously CP therapy has been used to treat both SARS
329 and MERS,(31) and currently can be rapidly deployed against SARS-CoV-2 while other therapies are
330 under development.(32) Nevertheless, many questions remain regarding the optimal antibody levels
331 necessary to treat patients at varying stages of COVID19 disease. Accurate quantification using serological

332 assays that predict neutralization activity may improve clinical outcomes through refinement of CP unit
333 selection for patients of varying symptomatology. In summary, we demonstrate that HTSA and S1 ELISA
334 assays show the strongest correlation with neutralization activity and may serve to predict the degree of
335 antiviral antibody activity present in recovered patients or vaccine recipients.
336

337 **Authors' Contributions**

338 LLL conceptualized the study, designed and performed serology experiments and managed the collection
339 of data, figures and statistical analyses. LLL, PB, TH and CDH co-wrote the manuscript. TH, PB, FM, YW
340 and FS designed and performed the neutralization assays. BR, DJ, WB, SJ, JP, MR and NT performed most
341 of the serology experiments. CG, MP, ES and HZ processed and preserved donor plasma and PBMCs. DS
342 coordinated donor demographic information. KY contributed to PBMC flow cytometry and interpretation.
343 DJ and BR contributed equal authorship to the manuscript. LLL, PB and TH contributed equal
344 corresponding authorship.
345

346 **Acknowledgements**

347 We thank Jill Alberigo, Amanda Brites and Kelly Brightman from Rhode Island Blood Center for their help
348 with performing the Ortho Anti-SARS-CoV-2 Total Test and the Abbott SARS-CoV-2 IgG test. We thank
349 Chockalingam Palaniappan and Paul Contestable for their assistance with performing the Ortho Anti-
350 SARS-CoV-2 IgG Test. We thank Haidee Chen for assistance with editing the manuscript.
351

352 **Conflicts of Interest**

353 The authors declare no conflicts of interest.
354

355 **Role of the Funding Source**

356 Funding source for TH, PBD, FM, YW and FS were NIH R01AI78788 and R37AI064003. Funding
357 sources did not have a role in the writing of the manuscript or the decision to submit for publication.

359 **Methods**

360 **Cell lines**

361 Huh7.5 cells were a gift from Charles Rice(33). The 293T/ACE2cl.13 cell clone was generated by
362 transducing 293T cells (ATCC® CRL-3216™) with a CSIB-based ACE2 lentivirus expression vector
363 containing a cDNA encoding a catalytically inactive ACE2 mutant. Single cell clones were isolated by
364 limiting dilution and one clone (293T/ACE2cl.13) was used in these studies.

365 **Collection of CP donor information, isolation of convalescent plasma and PBMCs**

366 Disclosure of demographic information was elective at the time of donation and showed that of the 370 CP
367 donors analyzed, 71.1% indicated age, 95.4% indicated blood type, 95.6% indicated sex and 55.1% indicated
368 ethnicity. To examine the demographic characteristics within the convalescent plasma (CP) donor population,
369 we used the 2010 U.S. Census demographic data as expected frequencies. Plasma was isolated from EDTA-
370 anticoagulated human whole blood samples. Samples were shipped from the NYBC Sample Management
371 Facility overnight at 4C and centrifuged for 5 min at 500 xg to facilitate plasma/cell phase separation. The
372 resulting upper plasma layer was extracted, aliquoted to minimize future freeze-thaw cycles, and stored at -
373 80 C. Samples were cryopreserved and stored in the NYBC COVID19 Research Repository
374 (https://nybc.org/covid19repository).

375 **Plasmid constructs**

376 The *env*-inactivated HIV-1 reporter construct (pHIV-1_{NL4-3} ΔEnv-NanoLuc) was generated from a pNL4-3
377 infectious molecular clone (obtained through NIH AIDS Reagent Program, Division of AIDS, NIAID, NIH
378 from Dr Malcolm Martin). It contains a NanoLuc Luciferase reporter gene in place of nucleotides 1-100 of
379 the *nef*-gene and a 940 bp deletion 3' to the *vpu* stop-codon. The rVSVΔG/NG/NanoLuc plasmid was
380 generated by insertion of a cassette containing an mNeonGreen/FMDV2A/NanoLuc luciferase cDNA into
381 rVSVΔG (Kerafast) (PMID: 20709108) between the M and L genes. The pSARS-CoV-2 S-protein
382 expression plasmid containing a C-terminally truncated SARS-CoV-2 S protein (pSARS-$CoV2_{\Delta 19}$) was
383 generated by insertion of a synthetic human-codon optimized cDNA encoding SARS-CoV-2 S1 spike protein
384 lacking the C-terminal 19 codons into pCR3.1. An ACE2 lentiviral expression vector was constructed by

385 inserting a cDNA encoding a catalytically inactive ACE2 mutant into the lentivirus expression vector CSIB
386 (PMID: 30084827).

387 **SARS-CoV-2 pseudotype particles**

388 To generate (HIV/NanoLuc)-SARS-CoV-2 pseudotype particles, 293T cells were transfected with pHIV-
389 1_{NL4-3} ΔEnv-NanoLuc reporter virus plasmid and pSARS-CoV-2-$S_{\Delta 19}$ at a molar plasmid ratio of 1:0.55. The
390 transfected cells were washed twice with PBS the following day, and at 48h after transfection, supernatant
391 was harvested, clarified by centrifugation, passed through a 0.22 µm filter, aliquoted and frozen at -80ºC.
392 To generate (VSV/NG/NanoLuc)-SARS-CoV-2 pseudotype particles, 293T cells were infected with
393 recombinant T7-expressing vaccinia virus (vTF7-3) and transfected with rVSVΔG/NG/NanoLuc, pBS-N,
394 pBS-P, pBS-L, and pBS-G (PMID: 20709108). At ~24h post transfection the supernatant was collected,
395 filtered and used to infect 293T cells transfected with a VSV-G expression plasmid, for amplification. To
396 prepare stocks of (VSV/NG/NanoLuc)-SARS-CoV-2 pseudotype particles, 293T cells were transfected with
397 pSARS-$CoV2_{\Delta 19}$ and infected with the VSV-G complemented rVSVΔG/NG/NanoLuc virus. At 16h later the
398 supernatant was collected, clarified by centrifugation, filtered, pelleted through a 20% sucrose cushion and
399 stored at -80ºC. The viral stock was incubated with 20% I1 hybridoma supernatant (ATCC CRL-2700) for
400 1h at 37ºC before use.

401 **Neutralization assays**

402 To measure neutralizing antibody activity in convalescent plasma, five-fold serial dilutions of plasma were
403 incubated for 1 hour at 37ºC in 96-well plates with an aliquot of HIV-1 or VSV-based SARS-CoV-2
404 pseudotyped virus containing approximately $1x10^3$ infectious units. Thereafter, 100 µl of the plasma/virus
405 mixture was added to target cells ($293T_{Ace2}$ cl.13, or Huh7.5) cells in 96-well plates. Cells were cultured for
406 48h (HIV-1 pseudotype viruses) or 16h (VSV pseudotype viruses). Then, cells were washed twice, lysed and
407 NanoLuc Luciferase activity in lysates was measured using either the Nano-Glo Luciferase Assay System
408 (Promega) and a Modulus II Microplate Multimode reader (Turner BioSystem) or a Glowmax Navigator
409 luminometer (Promega). The half maximal neutralizing titer (NT_{50}) for plasma, was determined using a 4-
410 parameter nonlinear regression in Prism 8.4 (GraphPad).

411 **Lateral Flow ImmunoAssay (LFA)**

412 Lateral flow immunoassays (LFAs) were provided by external companies. Assay cartridges contained
413 detection bands for IgG and IgM against SARS-CoV2 specific epitopes as well as an internal positive control.
414 For each assay, 20 µL convalescent plasma or serum was applied to the sample pad, followed by two drops
415 of proprietary running buffer. After 30 minutes, high resolution pictures of the detection zone were taken and
416 saved as .JPEG files. All tests were performed at room temperature.

417 **LFA Densitometry Analysis**

418 Relative quantification of anti-SARS-CoV-2 IgG and IgM in convalescent plasma samples was performed
419 using built-in gel analysis macros in FIJI (https://fiji.sc/). A rectangular selection covering the detection zone
420 was analyzed using Analyze>Gels>Plot Lanes. Integrated density values were outlined manually and
421 extracted from the resulting plot. Using MS Excel, IgG and IgM values were normalized against the density
422 of the control band.

423 The remaining whole blood cellular phase was supplemented with 2 mL of 35 g/L HSA/DPBS and diluted
424 1:1 with DPBS. Diluted whole blood was layered over 7 mL Ficoll-Paque Premium 1.078 g/mL (GE
425 Healthcare) and centrifuged for 20 minutes at 20C and 400xg without braking. Buffer coats were extracted,
426 counted with AOPI viability stain using the Cellometer Auto2000 (Nexelom Bioscience LLC), and frozen in
427 PBMC freezing media (10% DMSO in Knockout SR).

428 **SARS-CoV-2 Binding-Antibody ELISA**

429 Flat-well, nickel-coated 96 well ELISA plates (Thermo Scientific) were coated with 2µg/mL of recombinant
430 S1 spike protein, nucleocapsid protein, or Receptor Binding Domain (RBD) spike protein specific to SARS-
431 CoV-2 in resuspension buffer (1% Human Serum Albumin in 0.01% PBST) and incubated in a stationary
432 humidified chamber overnight at 4 C. On the day of the assay, plates were blocked for 30 min with ELISA
433 blocking buffer (3% W/V non-fat milk in PBST). Standard curves for both S1 and RBD assays were
434 generated by using mouse anti-SARS-CoV spike protein monoclonal antibody (clone [3A2], ABIN2452119,
435 Antibodies-Online) as the standard. Anti-SARS-CoV-2 Nucleocapsid mouse monoclonal antibody (clone
436 [7E1B], bsm-41414M, Bioss Antibodies) was used as a standard for nucleocapsid binding assays.

437 Monoclonal antibody standard curves and serial dilutions of convalescent donor plasma were prepared in
438 assay buffer (1% non-fat milk in PBST) and added to blocked plates in technical duplicate for 1 hr with
439 orbital shaking at room temperature. Plates were then washed three times with PBST and incubated for 1 hr
440 with ELISA assay buffer containing Goat anti-Human IgA, IgG, IgM (Heavy & Light Chain) Antibody-HRP
441 (Cat. No. ABIN100792, Antibodies-Online) and Goat anti-Mouse IgG2b (Heavy Chain) Antibody-HRP (Cat.
442 No. ABIN376251, Antibodies-Online) at 1:30000 and 1:3000 dilutions, respectively. Plates were then
443 washed three times, developed with Pierce TMB substrate for 5 min, and quenched with 3 M HCl.
444 Absorbance readings were collected at 450 nm. Standard curves were constructed in Prism 8.4 (Graphpad
445 Software Inc.) using a Sigmoidal 4PL Non-Linear Regression (curve fit) model.

446 **High-throughput Serology Assays**

447 Convalescent donor plasma samples were barcoded and dispatched to Rhode Island Blood Center (RIBC).
448 Samples were analyzed using the Abbott SARS-CoV-2 IgG chemiluminescent microparticle immunoassay
449 with the Abbott Architect *i*2000SR (Abbott Core Laboratories), as well as the VITROS Immunodiagnostic
450 Products Anti-SARS-CoV-2 Total Test and the Anti-SARS-CoV-2 IgG Test with the VITROS 5600 (Ortho
451 Clinical Diagnostics). All assays were performed by trained RIBC employees according to the respective
452 manufacturer standard procedures.

453 **Flow cytometric analysis of PBMCs**

454 Cryopreserved PBMCs were thawed, filtered and stained with a B-cell or T-cell antibody cocktail for 30
455 minutes in PBS. Cells were washed with PBS and analyzed with a BD LSR Fortessa 4 laser cytometer.
456 Cytometric analysis was performed using RUO FCS Express 7 (DeNovo Software).

457

458

459

460

461

462

References

1. F. Wu *et al.*, A new coronavirus associated with human respiratory disease in China. *Nature* **579**, 265-269 (2020).
2. P. Zhou *et al.*, A pneumonia outbreak associated with a new coronavirus of probable bat origin. *Nature* **579**, 270-273 (2020).
3. K. G. Andersen, A. Rambaut, W. I. Lipkin, E. C. Holmes, R. F. Garry, The proximal origin of SARS-CoV-2. *Nat Med* **26**, 450-452 (2020).
4. M. Xie, Q. Chen, Insight into 2019 novel coronavirus - An updated interim review and lessons from SARS-CoV and MERS-CoV. *Int J Infect Dis* **94**, 119-124 (2020).
5. Q. Yao *et al.*, Retrospective study of risk factors for severe SARS-Cov-2 infections in hospitalized adult patients. *Pol Arch Intern Med* 10.20452/pamw.15312 (2020).
6. A. J. Kucharski *et al.*, Early dynamics of transmission and control of COVID-19: a mathematical modelling study. *Lancet Infect Dis* **20**, 553-558 (2020).
7. C. M. Chan *et al.*, Examination of seroprevalence of coronavirus HKU1 infection with S protein-based ELISA and neutralization assay against viral spike pseudotyped virus. *J Clin Virol* **45**, 54-60 (2009).
8. C. Y. Lee, R. T. P. Lin, L. Renia, L. F. P. Ng, Serological Approaches for COVID-19: Epidemiologic Perspective on Surveillance and Control. *Front Immunol* **11**, 879 (2020).
9. X. Zhong *et al.*, B-cell responses in patients who have recovered from severe acute respiratory syndrome target a dominant site in the S2 domain of the surface spike glycoprotein. *J Virol* **79**, 3401-3408 (2005).
10. W. Tai *et al.*, Characterization of the receptor-binding domain (RBD) of 2019 novel coronavirus: implication for development of RBD protein as a viral attachment inhibitor and vaccine. *Cell Mol Immunol* 10.1038/s41423-020-0400-4 (2020).
11. L. A. VanBlargan, L. Goo, T. C. Pierson, Deconstructing the Antiviral Neutralizing-Antibody Response: Implications for Vaccine Development and Immunity. *Microbiol Mol Biol Rev* **80**, 989-1010 (2016).
12. DHHS, U.S. Census Bureau.
13. M. Hoffmann *et al.*, SARS-CoV-2 Cell Entry Depends on ACE2 and TMPRSS2 and Is Blocked by a Clinically Proven Protease Inhibitor. *Cell* **181**, 271-280 e278 (2020).
14. A. W. Fan Wu, Mei Liu, Qimin Wang, Jun Chen, Shuai Xia, Yun Ling, Yuling Zhang, Jingna Xun, Lu Lu, Shibo Jiang, Hongzhou Lu, Yumei Wen, Jinghe Huang, Neutralizing antibody responses to SARS-CoV-2 in a COVID-19 recovered patient cohort and their implications. *medRxiv* 10.1101/2020.03.30.20047365 (2020).
15. C. G. Davide F. Robbiani, Frauke Muecksch, Julio C. C. Lorenzi1 , Zijun Wang, Alice Cho, Marianna Agudelo, Christopher O. Barnes, Anna Gazumyan, Shlomo Finkin, Thomas Hagglof, Thiago Y. Oliveira, Charlotte Viant, Arlene Hurley, HansHeinrich Hoffmann, Katrina G. Millard, Rhonda G. Kost, Melissa Cipolla, Kristie Gordon,, S. T. C. Filippo Bianchini1, Victor Ramos, Roshni Patel, Juan Dizon, IrinaShimeliovich1, Pilar Mendoza, Harald Hartweger, Lilian Nogueira, Maggi Pack, Jill Horowitz, Fabian Schmidt, Yiska Weisblum, Eleftherios Michailidis, Alison W. Ashbrook, Eric Waltari,John E. Pak, Kathryn E. Huey-Tubman, Nicholas Koranda, Pauline R. Hoffman, Anthony P.West, Jr., Charles M. Rice, Theodora Hatziioannou, Pamela J. Bjorkman, Paul D. Bieniasz, Marina Caskey, Michel C. Nussenzweig, Convergent Antibody Responses to SARS-CoV-2 Infection in Convalescent Individuals. 10.1101/2020.05.13.092619. (2020).
16. C. P. Gross *et al.*, Racial and Ethnic Disparities in Population-Level Covid-19 Mortality. *J Gen Intern Med* 10.1007/s11606-020-06081-w (2020).
17. B. H. Shaz, A. B. James, K. L. Hillyer, G. B. Schreiber, C. D. Hillyer, Demographic patterns of blood donors and donations in a large metropolitan area. *J Natl Med Assoc* **103**, 351-357 (2011).
18. B. H. Shaz, C. D. Hillyer, Minority donation in the United States: challenges and needs. *Curr Opin Hematol* **17**, 544-549 (2010).
19. A. W. Fan Wu, Mei Liu, Qimin Wang, Jun Chen, Shuai Xia, Yun Ling, Yuling Zhang, Jingna Xun, Lu Lu, Shibo Jiang, Hongzhou Lu, Yumei Wen, Jinghe Huang, Neutralizing antibody responses to SARS-CoV-2 in a COVID-19 recovered patient cohort and their implications. 10.1101/2020.03.30.20047365.
20. M. J. Joyner *et al.*, Effect of Convalescent Plasma on Mortality among Hospitalized Patients with COVID-19: Initial Three-Month Experience. *medRxiv* 10.1101/2020.08.12.20169359 (2020).
21. P. Kellam, W. Barclay, The dynamics of humoral immune responses following SARS-CoV-2 infection and the potential for reinfection. *J Gen Virol* 10.1099/jgv.0.001439 (2020).
22. K. A. Callow, H. F. Parry, M. Sergeant, D. A. Tyrrell, The time course of the immune response to experimental coronavirus infection of man. *Epidemiol Infect* **105**, 435-446 (1990).
23. A. F. Bradburne, M. L. Bynoe, D. A. Tyrrell, Effects of a "new" human respiratory virus in volunteers. *Br Med J* **3**, 767-769 (1967).
24. M. Jaume *et al.*, Anti-severe acute respiratory syndrome coronavirus spike antibodies trigger infection of human immune cells via a pH- and cysteine protease-independent FcgammaR pathway. *J Virol* **85**, 10582-10597 (2011).
25. S. F. Wang *et al.*, Antibody-dependent SARS coronavirus infection is mediated by antibodies against spike proteins. *Biochem Biophys Res Commun* **451**, 208-214 (2014).
26. Y. Wan *et al.*, Molecular Mechanism for Antibody-Dependent Enhancement of Coronavirus Entry. *J Virol* **94** (2020).

27. A. Iwasaki, Y. Yang, The potential danger of suboptimal antibody responses in COVID-19. *Nat Rev Immunol* **20**, 339-341 (2020).
28. G. Marano *et al.*, Convalescent plasma: new evidence for an old therapeutic tool? *Blood Transfus* **14**, 152-157 (2016).
29. E. M. Bloch *et al.*, Deployment of convalescent plasma for the prevention and treatment of COVID-19. *J Clin Invest* 10.1172/JCI138745 (2020).
30. K. Duan *et al.*, Effectiveness of convalescent plasma therapy in severe COVID-19 patients. *Proceedings of the National Academy of Sciences of the United States of America* **117**, 9490-9496 (2020).
31. B. L. Brown, J. McCullough, Treatment for emerging viruses: Convalescent plasma and COVID-19. *Transfus Apher Sci* 10.1016/j.transci.2020.102790, 102790 (2020).
32. A. Budhai *et al.*, How did we rapidly implement a convalescent plasma program? *Transfusion* 10.1111/trf.15910 (2020).
33. K. J. Blight, J. A. McKeating, C. M. Rice, Highly permissive cell lines for subgenomic and genomic hepatitis C virus RNA replication. *J Virol* **76**, 13001-13014 (2002).

538 **Figure 1**

539

540

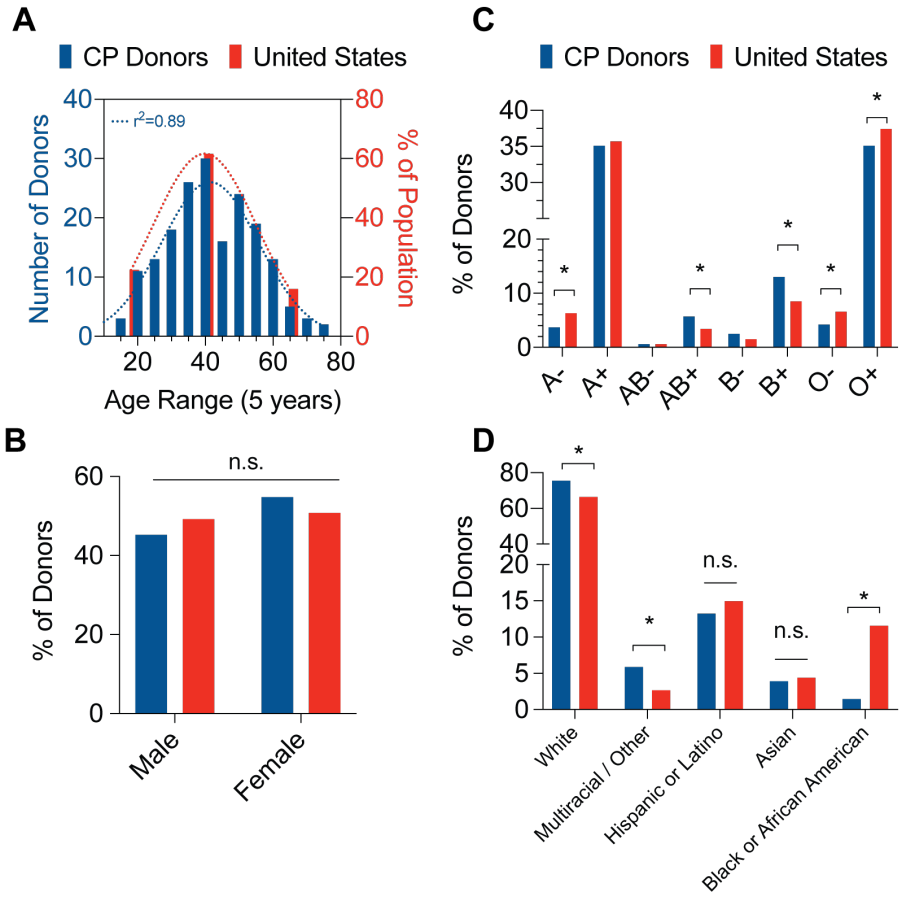

541

542

543 **Figure 2**
544

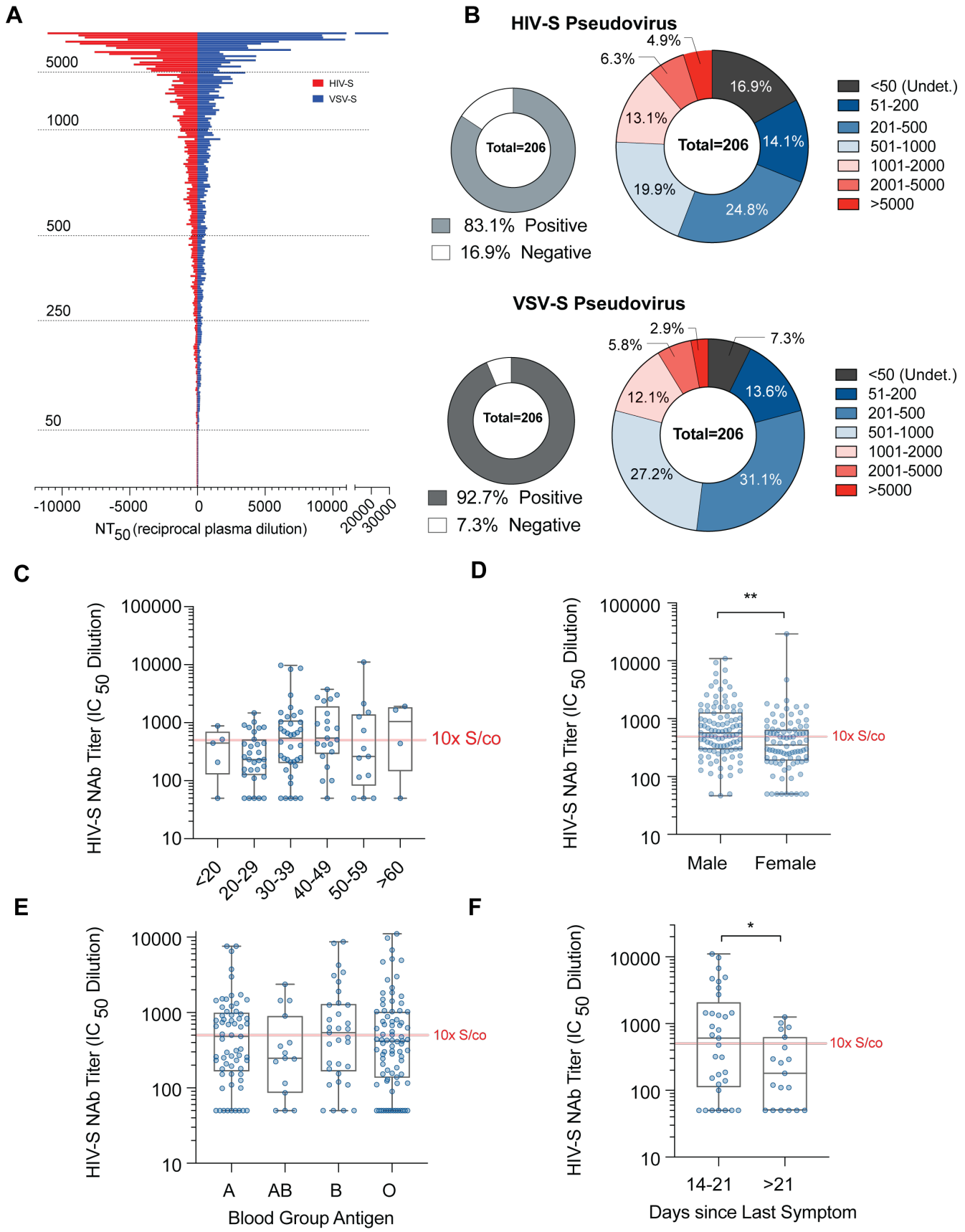

545
546
547

548 **Figure 3**

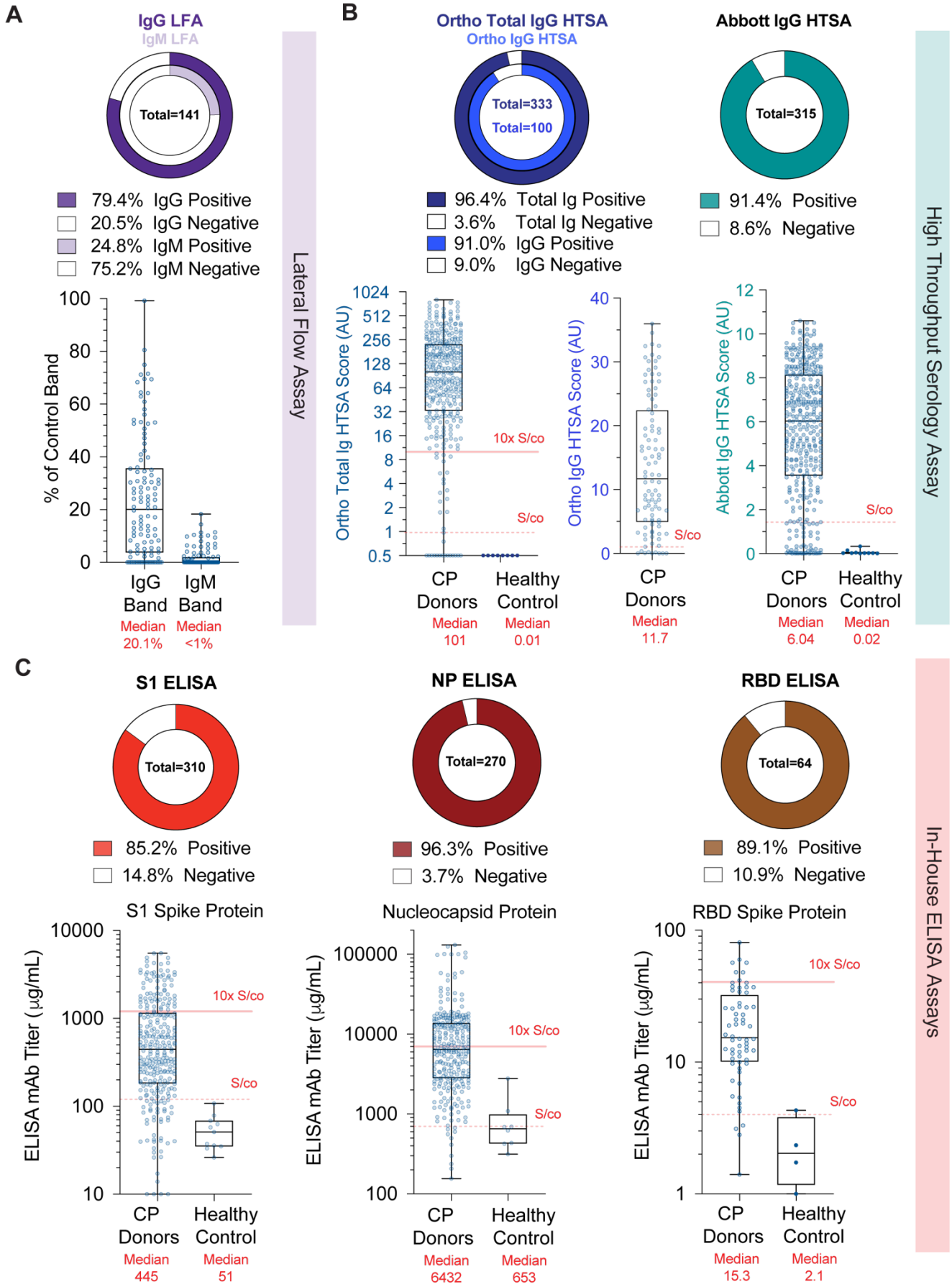

549
550
551

552 **Figure 4**

553

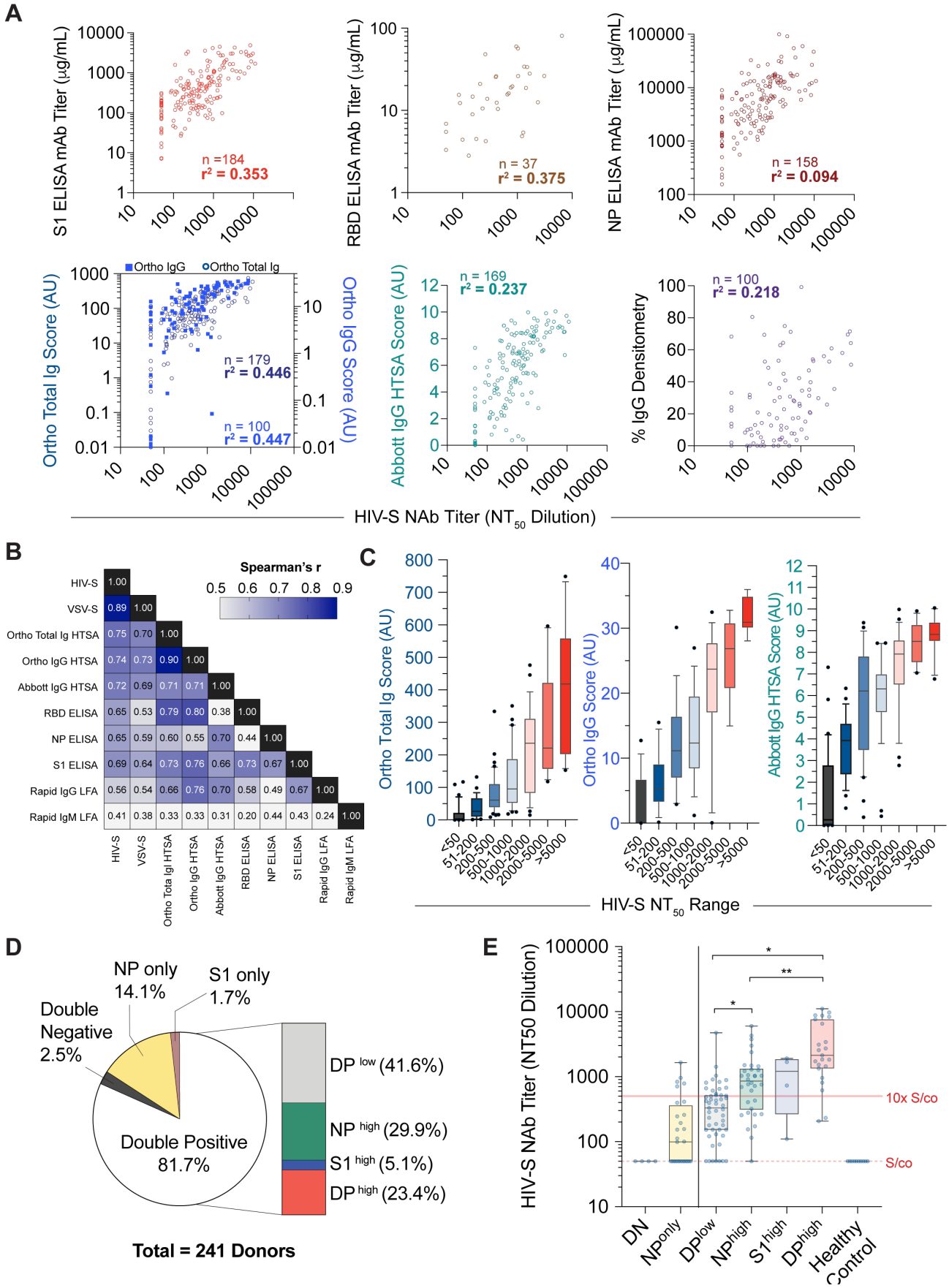

554

Figure 1: Demographics of convalescent plasma donors.

A; Distribution of convalescent plasma donor age (left, blue bars) compared to U.S. population (right, red bars). Dotted line represents Gaussian distribution curve fit. N=263; Pearson's correlation coefficient.

B; Distribution of convalescent plasma donor blood group antigen (left, blue bars) compared to U.S. population (right, red bars). N=370, binomial test for discrepancy versus U.S. population; * $p < 0.05$.

C; Distribution of convalescent plasma donor sex (blue bars) compared to U.S. population (red bars). N=354, binomial test for discrepancy versus U.S. population.

D; Distribution of convalescent plasma donor ethnicity (blue bars) compared to U.S. population (right, red bars). N=204, binomial test for discrepancy versus U.S. population; * $p<0.05$.

Figure 2: Neutralizing activity analysis of convalescent plasma donors.

A; Distribution of neutralization IC_{50} values (NT50, reciprocal plasma dilution) of convalescent donor plasma using HIV (red) or VSV pseudovirus (blue) overexpressing the SARS-CoV-2 spike protein (S).

B; Frequency of convalescent plasma donor NT50 values within indicated groups using HIV-S (top) or VSV-S pseudovirus constructs.

C; Frequency distribution of convalescent plasma HIV-S NT50 values versus age groups. Signal to cutoff (S/co, dotted grey line) and 10x S/co (solid grey line) thresholds are indicated. n=5-38, Kruskal-Wallis test; * $p < 0.05$.

D; Frequency of convalescent plasma donor NT50 values versus sex. Signal to cutoff (S/co, dotted grey line) and 10x S/co (solid grey line) thresholds are indicated. n=190, Mann-Whitney test, ** $p < 0.01$.

E; Frequency of convalescent plasma donor NT50 values versus blood group antigen. Signal to cutoff (S/co, dotted grey line) and 10x S/co (solid grey line) thresholds are indicated. n=15-82, Kruskal-Wallis test, * $p < 0.05$.

F; Frequency of convalescent plasma donor NT50 values versus time (days) since last reported symptom. Signal to cutoff (S/co, dotted grey line) and 10x S/co (solid grey line) thresholds are indicated. n=19-33, Mann-Whitney t-test, *$p < 0.05$.

592 **Figure 3: Serological analysis of convalescent plasma donors.**
593
594 **A;** Frequency of densitometric IgG (left) or IgM (right) results from LFA bands relative to control band.
595 Median values (red band) with 1st and 3rd quartiles (thin red lines) are shown.
596
597 **B;** Frequency of HTSA results using the total Ig or IgG assays derived from the Ortho Diagnostics platform
598 (left) or Abbott IgG assay platform (right). Results from fresh frozen plasma (FFP) units collected before
599 COVID19 are shown as healthy controls.
600
601 **C;** Frequency of S1 spike protein (left), Nucleocapsid (NP) protein (center) and RBD spike protein (right)
602 ELISA titer results. Titers reflect concentrations calculated using a mAb standard curve and not absolute
603 plasma concentrations. Median values (red band) with 1st and 3rd quartiles (thin red lines) are shown.
604

605 **Figure 4: Correlation of serology assays versus neutralization activity of convalescent plasma donors.**
606
607 **A;** Linear regression of HIV-S NT50 values (abscissa) versus serological assay values (ordinate). N
608 indicated in each graph, r^2 = goodness of fit.
609
610 **B;** Spearman correlation coefficients, *r*, of neutralization and serological assays. N=137 samples.
611
612 **C;** Distribution of CP donor sample HTSA scores within indicated HIV-S NT50 groups using Ortho total Ig
613 (left), Ortho IgG (center) or Abbott IgG (right) assays.
614
615 **D;** Frequency of convalescent donor S1 and NP ELISA values defined in **C**. n=241 samples.
616
617 **E;** Distribution of NT50 values corresponding to populations defined in **C**. n=4-51, Kruskall-Wallis test, *
618 $p < 0.05$, ** $p < 0.01$.
619